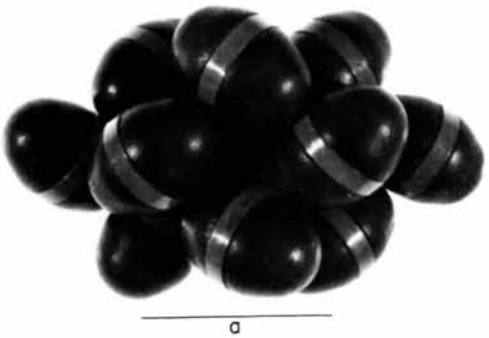


Fig. 11. Cubic *Pa*3 structure simulating the crystal structure of acetylene at high temperatures.

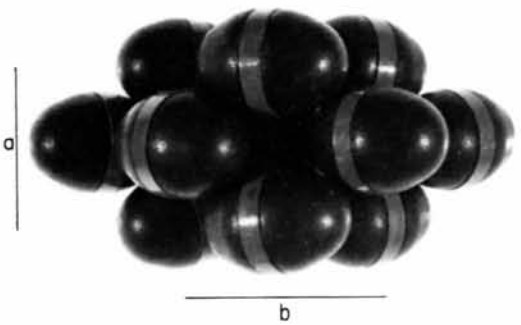


Fig. 12. Orthorhombic *Cmca* structure simulating the crystal structure of acetylene at low temperatures.

than at low temperatures. The high-temperature structure of solid acetylene is in fact cubic *Pa*3, the characteristic structure into which quadrupolar spheres are assembled. This cubic structure (Fig. 11) can change to *Cmca* (Fig. 12) by rotation of the molecules through an angle 45°, whereas the rotation of some molecules through 90° is necessary for the transition to *Pnnm* (compare Fig. 11 and Fig. 12 in part II). The barrier to *Cmca* is possibly lower, thus favouring the transition to this structure.

A unit cell of the *Cmca* structure in which our molecular models are assembled has the ratios $a/c = 0{\cdot}85$ and $b/c = 0{\cdot}95$, which correspond to $a/c = 0{\cdot}896$ and $b/c = 0{\cdot}970$ observed by Koski & Sándor (1975).

One of the authors (TK) thanks Dr H. K. Koski for useful information. Thanks are due to Dr K. Miyoshi for valuable advice on the display of charge-density contours.

### References

BADER, R. F. W., HENNEKER, W. H. & CADE, P. E. (1967). *J. Chem. Phys.* **46**, 3341–3363.
KIHARA, T. (1963). *Acta Cryst.* **16**, 1119–1123.
KIHARA, T. (1966). *Acta Cryst.* **21**, 877–879.
KIHARA, T. (1970). *Acta Cryst.* A**26**, 315–320.
KIHARA, T. (1975). *Acta Cryst.* A**31**, 718–721.
KOSKI, H. K. & SÁNDOR, E. (1975). *Acta Cryst.* B**31**, 350–353.
SNYDER, L. C. & BASCH, H. (1972). *Molecular Wave Functions and Properties*. New York: John Wiley.
TURNER, A. G., SATURNO, A. F., HAUK, P. & PARR, R. G. (1963). *J. Chem. Phys.* **40**, 1919–1928.

*Acta Cryst.* (1978). A**34**, 329–336

## Elimination of Extinction by a Temperature Gradient

BY PAUL SEILER AND JACK D. DUNITZ

*Organic Chemistry Laboratory, Swiss Federal Institute of Technology, ETH-Zentrum,* 8092 *Zürich, Switzerland*

(*Received* 7 *October* 1977; *accepted* 5 *November* 1977)

Experiments with crystals of a $KNCS.C_{12}H_{24}O_6$ complex show that the integrated intensities of reflections showing strong extinction can be raised to their expected kinematic values when the crystal is subjected to a temperature gradient. The intensity increases are accompanied by a broadening of the diffraction peaks and are reversible with no detectable hysteresis. These observations seem to be incompatible with the mosaic-crystal model. Local variations in the extinction behaviour have been detected by using a fine incident beam and suggest inhomogeneity of crystal texture. The intensity increases are probably connected with a reduction in the mean size of the perfect crystal domains, *i.e.* with a decrease of the mean spatial correlation length within the crystal.

### Introduction

Extinction is one of the most serious problems in accurate X-ray diffraction intensity measurements. The present paper describes some experiments that bear on this problem. It is shown that application of a temperature gradient (TG) to a crystal during the diffraction process can reduce, or in some cases even eliminate,

extinction errors. The intensity changes produced by applying or removing the TG are reversible, an observation which is difficult to reconcile with the usual mosaic model of an imperfect crystal.

Before discussing the experiments in detail, we shall review briefly the present status of the extinction problem. The theoretical aspects of extinction have been extensively discussed during the last 10 years. Zachariasen (1967) put forward a 'general theory' of X-ray diffraction from crystals, leading to a formula for the integrated intensity that was claimed to be valid over the entire range from the perfect to the ideal mosaic crystal. The Zachariasen theory is essentially based on the kinematic approximation and the usual mosaic model (Darwin, 1922) of the imperfect crystal. However, in his treatment of secondary extinction, Zachariasen distinguishes two types of imperfect crystal: type I, where extinction depends mainly on $g$, a quantity inversely proportional to the mosaic spread, and type II, where extinction depends mainly on $r$, the mean radius of the mosaic blocks. Primary extinction is also allowed for if $r$ is large ($>10^{-4}$ cm). In addition to an extension by Coppens & Hamilton (1970) to cover anisotropic extinction, the theory has been significantly improved for the case of strong extinction (Cooper & Rouse, 1970; Becker & Coppens, 1974) and adapted for use in least-squares refinement of crystal structures, from which values of $r$ and $g$ may be estimated. However, as Lawrence (1977) has pointed out, 'reasonable' estimates of these parameters do not necessarily justify the conclusion that the underlying mosaic model is physically realistic. The interpretation is especially problematic when primary extinction has to be allowed for.

In this connection, it must be mentioned that the distinction between primary and secondary extinction (or between coherent and incoherent scattering) is somewhat arbitrary with reference to real, imperfect crystals. Kato (1976) considers that if a mean correlation length within the crystal is larger than a critical distance $\Lambda$ (equal to the primary extinction distance or *Pendellösung* fringe spacing in order of magnitude) then a wave-optical treatment of the problem is to be preferred to the kinematical approach. The wave-optical treatment would also be preferable for dealing with certain kinds of crystal distortion. This would require that the defect structure of each investigated crystal specimen be known in detail, which is rather the exception than the rule today.

There is obviously a need for an experimental method for determining the true kinematic value of the structure factors, and several approaches have been proposed. These involve the use of a plane-polarized incident beam (Chandrasekhar, 1956; Chandrasekhar, Ramaseshan & Singh, 1969) or intensity measurements at several wavelengths and extrapolation to zero wavelength (Lawrence, 1977) or combinations of these (Mathieson, 1977). The approach described in this paper differs radically from any of these.

### Preliminary observations

In the course of some routine diffractometer measurements, curious fluctuations in the intensities of certain reflections were observed. The crystal under study was the potassium thiocyanate complex with 1,4,7,10,13,16-hexaoxacyclooctadecane(18-crown-6), $KNCS.C_{12}H_{24}O_6$, monoclinic, $P2_1/c$, $a = 8{\cdot}190$, $b = 14{\cdot}285$, $c = 7{\cdot}775$ Å, $\beta = 99{\cdot}19°$ (at room temperature), $Z = 2$. The $K^+$ ion occupies a crystallographic centre of symmetry, and the thiocyanate anions are disordered and interact only weakly with the complexed cations. A detailed description of the structure has been published (Seiler, Dobler & Dunitz, 1974).

A single crystal (obtained from ethanol/hexane) was cut with a razor blade to approximately 0·35 mm along each edge and attached to a glass fibre with Araldite. It was mounted with its unique axis (**b**) along the rotation axis $\omega$ of a Stoe two-circle diffractometer. When the crystal was oriented to produce the strong 040 reflection ($F_c = 74{\cdot}7$) with Mo $K\alpha$ radiation (monochromatized by reflection from graphite) and with crystal and counter both stationary, considerable fluctuations of the diffracted intensity were observed (Fig. 1, curve $A$). The possibility that these fluctuations were due to instrumental instabilities could soon be eliminated, but it was noticed that even greater intensity fluctuations could be produced by a gentle stream of warm air directed at the crystal (Fig. 1, curve $B$). No phase change occurs under these conditions.

By systematic variation of the experimental conditions, it was eventually concluded that the observed intensity fluctuations were associated with small temperature fluctuations in the air-conditioned laboratory. They disappear when the crystal is at thermal equilibrium. Analogous observations were made by Izrael & Petroff (1973), who noted that random fluctuations in

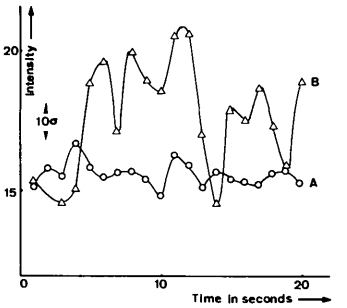


Fig. 1. Observed fluctuation of the diffracted intensity of the 040 reflection with crystal and counter stationary. $A$ under normal operating conditions; $B$ when a stream of warm air was directed at the crystal.

room temperature are enough to blur the *Pendellösung* fringes on X-ray topographs of triglycine sulphate. In both cases, small elastic disturbances of the crystal perfection must be involved.

### Qualitative observations

With the crystal in equi-inclination setting, the amplitude of the intensity fluctuations was observed to depend on the azimuthal angle $\psi$ (identical with rotation angle $\omega$ for this geometry). The integrated intensity of the 040 reflection, measured at different azimuthal angles, by manual step-scan with respect to $\mu$, also depends on $\psi$ (Fig. 2, curve *A*). The variation with $\psi$ is much too large to be explainable by normal absorption. The nearly flat $\psi$ profile of the weak 080 reflection (Fig. 2, curve *D*) suggests that it is rather an expression of anisotropic extinction. Similar examples have been discussed by Denne (1972) and especially by Thornley & Nelmes (1974).

In examining the influence of various experimental conditions we decided to investigate the behaviour of the $\psi$ profile when a constant TG was applied to the crystal. The results (Fig. 2, curves *B* and *C*) show clearly that the profile changes; the largest change is a marked increase in integrated intensity over a region around $\psi \sim 90$–$160°$. This is the same region where the largest intensity fluctuations were observed under normal operating conditions, *i.e.* in the absence of an applied TG. The other strong $0k0$ reflections show very similar $\psi$ profiles and similar changes on application of a TG. On removal of the TG, the integrated intensities fall back to their original values without detectable hysteresis, and the whole process can be repeated indefinitely. However, the direction of the TG is important. In these preliminary experiments, large intensity changes were produced when the TG was approximately parallel to **b**, *i.e.* approximately normal to $\mathbf{S}_0$ in the equi-inclination geometry. A TG normal to **b** and to $\mathbf{S}_0$ has very little effect. Batterman (1964) has shown that the diffracted intensities from a perfect crystal of Ge are influenced by the direction of heat flow within the crystal.

In these experiments (and in those described later) the TG was produced by directing two fine streams of cold and warm nitrogen at opposite sides of the crystal (Fig. 3). The measured temperature difference $\Delta T$ (referred to in the figures and tables) is the difference between the temperatures of the two gas streams as they left the jets. The actual temperature difference $\Delta T'$ between the two sides of the crystal is unknown but it must be much smaller than $\Delta T$. The mean temperature at the crystal was maintained at approximately 293 K.

Experiments with several crystal specimens of the same compound showed that the $\psi$ profiles of strong reflections are also very sensitive to mechanical strains produced, for example, by cutting and mounting the crystal. In the absence of a TG, the ratio of maximum to minimum intensity in the 040 $\psi$ profile was found to vary from about 1:1 to 2:1 for specimens cut to an

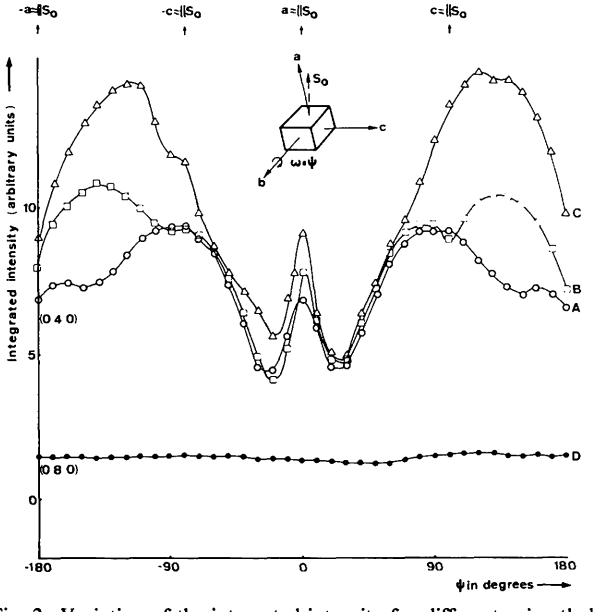


Fig. 2. Variation of the integrated intensity for different azimuthal angles $\psi$ (for $\psi = 0$, **a** is approximately parallel to $\mathbf{S}_0$). *A* 040 reflection with $\Delta T = 0$; *B* 040 reflections with $\Delta T \sim 7$ K; *C* 040 reflection with $\Delta T \sim 20$ K; *D* 080 reflection with $\Delta T = 0$.

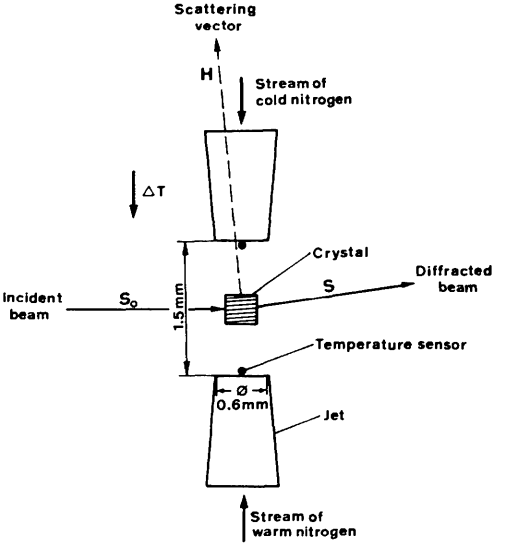


Fig. 3. Schematic representation of the device for producing a TG. In most of our experiments the TG was in the plane of **S** and $\mathbf{S}_0$ and perpendicular to $\mathbf{S}_0$. The measured temperature difference $\Delta T$ is the difference between the temperatures of the two streams of nitrogen as they left the jets. The mean temperature of the crystal was held constant at approximately 293 K.

approximately uniform shape. By avoiding mechanical treatment of any kind (uncut crystal adhering to Si grease, enclosed in a glass capillary), a practically flat $\psi$ profile could be obtained in the absence of a TG. Under these conditions, the extinction is nearly isotropic but also more severe than for cut and normally mounted crystals.

We conclude that the variations in the $\psi$ profiles produced by cutting and normal mounting are due mainly to inhomogeneous mechanical destruction of crystal perfection and are hence better discussed in terms of anisotropic primary extinction rather than secondary extinction. The reversibility of the intensity changes produced by a TG would point in the same direction.

### Thermal expansion

Fig. 2 (curves *B* and *C*) shows that the influence of a constant TG on the integrated intensity of the 040 reflection is strongly dependent on the azimuthal angle $\psi$. This dependence is connected with the strongly anisotropic thermal expansion of the crystal. Values of the thermal expansion coefficient $\alpha$ along various directions, determined within the temperature range 100 to 293 K, are:*

$$\begin{aligned}
\alpha(100) &\sim 18 \times 10^{-6}\ \mathrm{K}^{-1}\\
\alpha(010) &\sim 57 \times 10^{-6}\\
\alpha(001) &\sim 100 \times 10^{-6}\\
\alpha(\bar{1}01) &\sim 100 \times 10^{-6}\\
\alpha(101) &\sim 10 \times 10^{-6}.
\end{aligned}$$

Since **c** lies between **H**(001) and **H**($\bar{1}$01), it runs roughly parallel to the direction of maximum thermal expansion. There is a large change in $\beta$ of the unit cell ($\partial\beta/\partial t \sim 0{\cdot}005$ deg $\mathrm{K}^{-1}$). For technical reasons, the experiments described in this section are restricted to the behaviour of *h*0*l* reflections.

For this purpose, the direction of the TG was rotated by 90° about $\mathbf{S}_0$ to run normal to **b** and thus approximately parallel to the diffraction vector **H** for low-order *h*0*l* reflections. With this arrangement, the most striking intensity increases, *i.e.* the largest reductions in extinction, were observed for the strong low-order *h*00 reflections – produced when **c** was approximately parallel to $\mathbf{S}_0$ and thus perpendicular to the TG. It should be noted that for the 040 reflection, the greatest increase in intensity was also obtained with $\mathbf{S}_0$ approximately parallel to the direction of largest thermal expansion (Fig. 2).

These observations can be interpreted as follows. When the crystal is subjected to a TG, lattice nets perpendicular to the TG become curved because of the unequal thermal expansion in different parts of the crystal. The amount of curvature depends mainly on the thermal expansion coefficients in the plane perpendicular to the TG, as indicated schematically in Fig. 4. An additional deformation of the lattice nets occurs because of the large temperature dependence of $\beta$. The total lattice deformation of a given lattice net thus depends on the crystal orientation and will be greatest when the direction of maximum thermal expansion is perpendicular to the TG. We may assume that this lattice deformation destroys the exact regularity in phase of the radiation scattered at different parts of the crystal, which is necessary for primary extinction.

This would imply that the intensity increase caused by a TG should be accompanied by a broadening of the diffraction peak, as is indeed observed (Fig. 5). The broadening effect is reversible – but only up to a certain $\Delta T$ beyond which the elastic behaviour of the crystal is destroyed.

Quantitative calculations of the curvatures of net

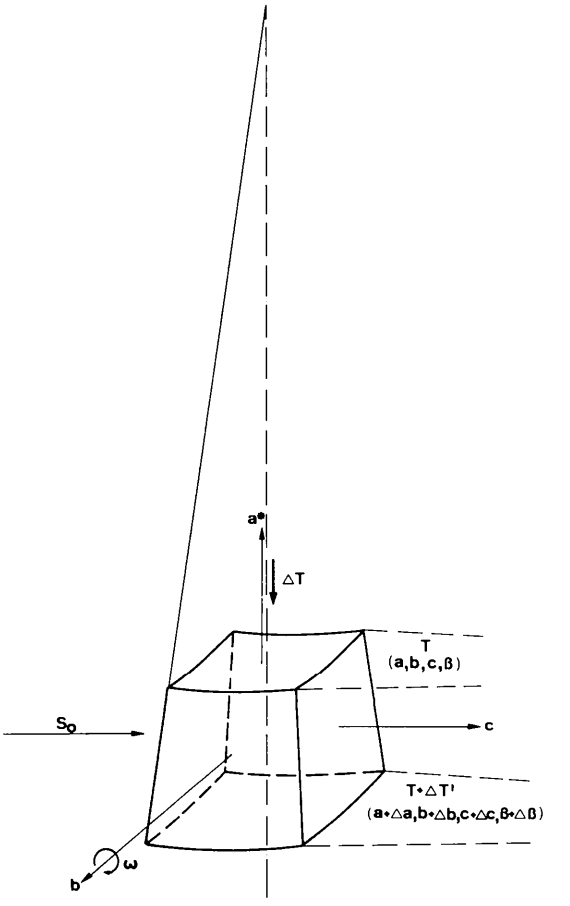


Fig. 4. Schematic representation of the bending of a crystal, when a TG is applied normal to $\mathbf{S}_0$ and **b**. The total lattice deformation depends on the amount of the crystal bending and on the deformation caused by the change of the $\beta$ angle of the unit cell.

* The structure analysis (Seiler, Dobler & Dunitz, 1974) showed that the vibrational ellipsoid of the $K^+$ ion is quite anisotropic. The direction of greatest thermal expansion is approximately parallel to the long axis of the ellipsoid.

planes caused by thermal gradients have been made by Penning & Polder (1961) and by Izrael & Petroff (1973). The influence of such lattice deformation on the integrated intensity has been discussed by Katagawa & Kato (1974).

### The approach to kinematic intensity

If the intensity increases on applying a TG are indeed caused by a reduction of extinction, then we might hope, by suitable choice of experimental conditions, to raise the diffracted intensity $P$ of an extinction-affected reflection to its kinematic value $P_k$, but no higher.

A detailed study has been made of the behaviour of the 100 reflection, with extinction factor $y \equiv P/P_k$ of

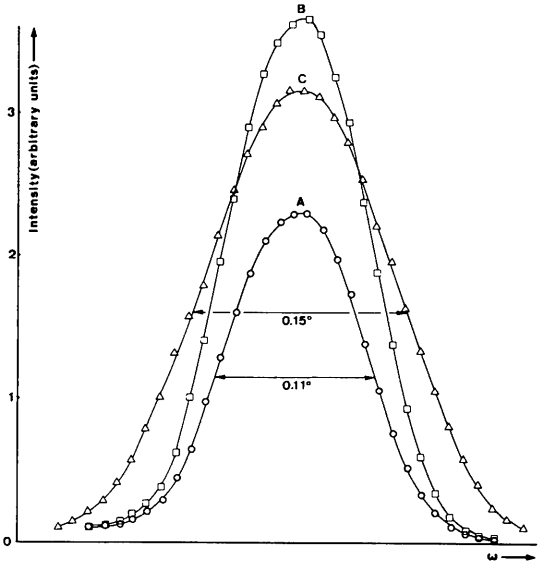


Fig. 5. Change of the profile of the 100 reflection peak with increasing $\Delta T$ ($\omega$ scan, Mo $K\alpha$ radiation). $A$ with $\Delta T = 0$; $B$ with $\Delta T \sim 5$ K; $C$ with $\Delta T \sim 50$ K. On removal of the TG, both the integrated intensity and the peak profile are indistinguishable from those of the original state of the crystal (curve $A$).

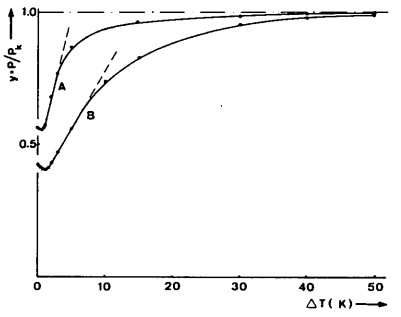


Fig. 6. Approach of the integrated intensity $P(100)$ to the expected kinematic intensity $P_k(100)$ with increasing $\Delta T$. $A$ for Mo $K\alpha$ radiation, $B$ for Cu $K\alpha$ radiation.

0·55 for Mo $K\alpha$ and 0·42 for Cu $K\alpha$ radiation. This reflection was judged especially suitable for detailed study because appreciable intensity changes can be produced by modest TG's.

Fig. 6 shows the behaviour of $y(100)$ as function of $\Delta T$ for Mo $K\alpha$ and Cu $K\alpha$ radiation. The kinematic intensity $P_k(100)$ was estimated from the value of $F_c(100)$ based on the previous structure analysis (Seiler, Dobler & Dunitz, 1974). The scale factor was obtained by comparing observed intensities $P_1$ of 15 weak, extinction-free $h0l$ reflections with values $P_o$ derived from corresponding $F_o$ values. $R = \Sigma|kP_1 - P_o|/\Sigma P_o$ was 0·025.

From Fig. 6, it can be seen that not only is the extinction factor $y$ for Cu $K\alpha$ radiation smaller at $\Delta T = 0$, but it also approaches unity more slowly with increasing $\Delta T$. The slight dips in the curves at small $\Delta T$ are reproducible. They suggest that strain, probably of mechanical origin, is already present in the absence of a TG and that this strain opposes the strain induced by the TG. In both curves, the dip is followed by a more or less linear region; here the slope $dP/d(\Delta T)$ for Mo radiation is roughly double that for Cu radiation, *i.e.* roughly inversely proportional to $\lambda$. The curves then tend asymptotically to $y = 1$, whereby it must be noted that the effective temperature difference $\Delta T'$ between the ends of the actual crystal can hardly be expected to be proportional to $\Delta T$ over the entire range. Moreover, since the elastic properties of the crystal are unknown, it is uncertain whether or to what extent the crystal bending is homogeneous and within what range it is proportional to $\Delta T$.

Our crystals are certainly not ideally perfect. If any confirmation of this were needed, it comes from the observed intensities of the weak reflections, which show no systematic deviations from calculated $P_k$ values. Although the extinction behaviour of our crystals can probably by analysed in terms of the mosaic-crystal model, we do not believe that the resulting parameters would be physically meaningful; the reversibility of the phenomena described here more or less excludes all models of the mosaic type. We therefore tend rather to discuss the results in terms of the more general formulation of Kato (1976), which introduces a mean spatial correlation length $\tau$ to characterize the crystalline medium. The two extremes, $\tau \gtrsim$ crystal size and $\tau \sim 0$, correspond to ideally perfect and ideally imperfect crystals. Primary extinction will occur when $\tau$ is greater than the primary extinction distance $\Lambda$, which can be defined in slightly different ways (Kato, 1976; Becker, 1977) but is of the order of magnitude of

$$\Lambda = \frac{1}{r_e k\lambda}\left(\frac{V}{F_H}\right) = \left(\frac{\lambda}{Q_H \sin 2\theta}\right)^{1/2} \qquad (1)$$

where $r_e$ is the 'classical radius of the electron' ($2{\cdot}83 \times 10^{-13}$ m), $k$ is the polarization factor, and the other

symbols have their usual meanings:

$$Q_{\mathbf{H}} = \left(\frac{r_e k F_{\mathbf{H}}}{V}\right)^2 \frac{\lambda^3}{\sin 2\theta}. \qquad (2)$$

One may thus interpret Fig. 6 as an expression of the decrease of this correlation length within the crystal with increasing $\Delta T$.

### Inhomogeneity of crystal texture

For the 100 reflection the primary extinction distance $\Lambda$ (equation 1) is about 0·07 mm for Mo $K\alpha$ radiation [$F_c(100) = 63{\cdot}7$, $V = 898$ Å$^3$]. In order to gain an impression of local variations in the degree of crystal perfection, the diameter of the primary beam was reduced from 0·8 mm to about 0·02 mm by modifying the collimation system. By making small translations of the crystal perpendicular to the primary beam, six different crystal regions were sampled. For each region, an $\omega$ scan of the diffracted intensity 100 was made with $\Delta T \sim 50$ K (for which extinction is practically eliminated – see Fig. 6) as well as with $\Delta T \sim 0$. With $\Delta T \sim 50$ K, the integrated intensities from individual regions were equal to within a few percent, whereas with $\Delta T = 0$ the integrated intensity varied considerably from one region to another. Quantitative comparison of the integrated intensities measured under the two conditions led to $y$ values between 0·44 and 0·64; the mean value over the entire crystal with the wide beam is 0·55 (Fig. 6). Rocking curves, obtained by means of a $\gamma$-ray diffractometer from large imperfect single crystals, show that inhomogeneous crystal textures (and thus inhomogeneous extinction properties) are not unusual (Schneider, 1977).

With Mo $K\alpha$ radiation, extinction is largely eliminated with $\Delta T \sim 5$ K. Thereafter, the integrated intensity increases only very slowly, as already noted in Fig. 6, curve $A$. The behaviour of the $\omega$ profile with increasing $\Delta T$ was studied for the region showing the greatest extinction ($y = 0{\cdot}44$). Fig. 7 shows that although the integrated intensity is roughly the same for small and for large $\Delta T$, the $\omega$ profile is much broader (and the peak height correspondingly lower) in the latter case.* For some regions, a detectable splitting of the peak was observed (Fig. 7). This could suggest that such regions, which seem to behave as coherent domains in the absence of strain, can be separated into two components by thermal strain – and indeed in an elastic fashion, for, on removal of the TG, both the integrated intensity and the peak profile are indistinguishable from those of the original state of the crystal. It is difficult to see how this result can be interpreted in terms of the traditional mosaic-crystal model.

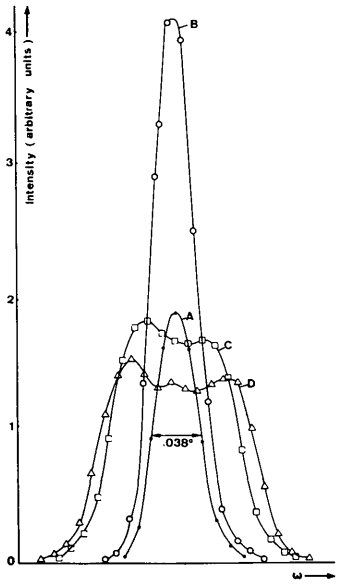


Fig. 7. Elastic splitting of the diffracton peak 100 with increasing $\Delta T$ ($\omega$ scan, Mo $K\alpha$ radiation). The diameter of the primary beam was reduced to about 0·02 mm for this experiment. The observed peak width of 0·038° at $\Delta T = 0$ is almost entirely accounted for by the width of the primary beam measured at the counter. $A$ with $\Delta T = 0$, integrated intensity $I = 8064$; $B$ with $\Delta T \sim 5$ K, $I = 16\,609$; $C$ with $\Delta T \sim 40$ K, $I = 18\,183$; $D$ with $\Delta T \sim 50$ K, $I = 18\,118$.

### Elimination of extinction

The previous results with individual reflections motivated us to attempt to eliminate extinction errors in general with a TG. For this purpose, a somewhat larger crystal, about 0·5 mm on edge, was selected and mounted uncut as described earlier so as to avoid mechanical strain. For technical reasons connected with the use of the two-circle diffractometer, we restricted ourselves to the $h0l$ reflections (the crystal was mounted as before with **b** parallel to the rotation axis $\omega$), which include the two strongest reflections $10\bar{2}$ and 100. The expected kinematic intensities $P_k$ were estimated as described earlier. In this connection, it was important to keep the mean temperature of the crystal constant at 293 K to avoid changes in the temperature factors. As checks, we used the strongly temperature-dependent $\beta$ angle as well as the intensities of a few high-order reflections. Moreover, for this set of experiments, the TG device was slightly modified to allow the direction of the TG to be rotated about the $\omega$-axis of the diffractometer.

The integrated intensities ($\omega$-scan, Mo $K\alpha$-radiation)

* Observed peak widths at $\Delta T = 0$ are virtually equal to the width of the reduced primary beam measured at the counter. The intrinsic mosaic spread of the crystal (at $\Delta T = 0$) must be at least an order of magnitude smaller than the width of the $\omega$ profile shown in Fig. 7 (curve $A$).

of the 15 strongest *h*0*l* reflections, measured with and without a TG, are listed in Table 1, together with their expected kinematic intensities $P_k$. The results are summarized in Fig. 8, which shows that extinction has practically been eliminated by applying the TG.

It has to be admitted that the nearly 300% increase in $P(10\bar{2})$ [$\Delta(10\bar{2}) \sim 0{\cdot}03$ mm] was only achieved with some effort. For this reflection, when the TG is perpendicular to $\mathbf{S}_0$ [*i.e.* nearly parallel to $\mathbf{H}$ $(10\bar{2})$] it happens to be also perpendicular to a direction of relatively small thermal expansion. With this arrangement, it was not possible to increase $y$ to more than about 0·6, even with $\Delta T$ as great as 250 K. By rotating the TG about $\omega$, it could be brought into a direction nearly perpendicular to the direction of maximum thermal expansion. With this arrangement, $y$ could be increased from 0·25 to 0·94 with a concomitant widening of the reflection peak at half-height by about 0·7°. In contrast to the usual behaviour, the return to the initial state of the crystal on removal of the TG was slow and still incomplete ($y \sim 0{\cdot}35$) even after several hours. It seems clear that, for this reflection and for this particular crystal specimen, we are on the limit of applicability of the TG method. On applying still larger TG's, more pronounced inelastic deformations of the crystal tend to occur; in other words, the crystal tends to shatter. With smaller specimens, the extinction of the $10\bar{2}$ reflection could be completely eliminated.

Table 1. *List of the expected kinematic intensities $P_k$ of the 15 strongest h0l reflections, together with their integrated intensities P (ω scan, Mo Kα radiation) measured with and without a TG*

| *h* | *k* | *l* | $P_k$ | *P* with TG | *P* without TG |
|---|---|---|---|---|---|
| 1 | 0 | $\bar{2}$ | 155903 | 146550 | 39350 |
| 1 | 0 | 0 | 46049 | 45665 | 18109 |
| 2 | 0 | $\bar{2}$ | 14674 | 14107 | 10324 |
| 3 | 0 | 0 | 9571 | 8691 | 6446 |
| 4 | 0 | $\bar{2}$ | 6042 | 6110 | 4953 |
| 4 | 0 | 2 | 2408 | 2306 | 2171 |
| 3 | 0 | $\bar{2}$ | 1593 | 1544 | 1466 |
| 0 | 0 | 2 | 1475 | 1401 | 1343 |
| 5 | 0 | $\bar{2}$ | 1470 | 1443 | 1391 |
| 2 | 0 | 4 | 1450 | 1456 | 1367 |
| 2 | 0 | $\bar{4}$ | 1381 | 1455 | 1407 |
| 5 | 0 | 0 | 1083 | 1047 | 1036 |
| 3 | 0 | $\bar{4}$ | 1011 | 954 | 922 |
| 5 | 0 | 2 | 944 | 922 | 916 |
| 1 | 0 | $\bar{4}$ | 883 | 922 | 907 |

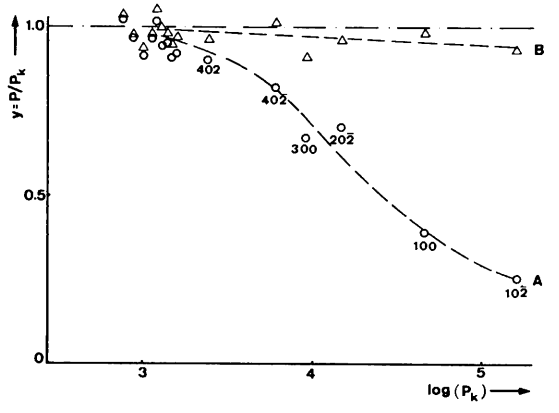


Fig. 8. Extinction behaviour of the 15 strongest *h*0*l* reflections. *A* with $\Delta T = 0$, *B* with $\Delta T$ ranging from 100 to 250 K, depending on the reflection and crystal orientation. The average temperature was maintained constant at 293 K.

## Conclusions

It has been shown that extinction can be eliminated or at least drastically reduced by aplying a TG to the crystal. The effect depends on the magnitude and direction of the TG as well as on the elastic properties and thermal-expansion behaviour of the crystal. Our experience is that, with a constant TG, best results for low-order reflections are obtained with the TG in the plane of $\mathbf{S}$ and $\mathbf{S}_0$ and perpendicular to the direction of maximal thermal expansion in this plane. However, we have not studied all the factors that may be involved. The stronger the extinction, the more difficult it is to eliminate. The prospect of eliminating extinction, rather than just reducing it, is therefore obviously improved by using as small a wavelength and as small a crystal as possible. Quite apart from its possible usefulness in correcting for extinction, the method described here seems well suited to obtaining information about the nature of the extinction phenomenon. In particular, our results suggest that the role of primary extinction is often underestimated in the analysis of extinction effects from crystals of typical size (linear dimensions ~0·03 cm) used in X-ray diffractometry.

As mentioned earlier, the experiments described in this paper were all carried out with crystals of the KNCS complex of 18-crown-6. However, similar results have been obtained with other organic and organometallic crystals showing severe extinction.

The work described in this paper was not carried out as part of a systematic study of the extinction problem. The initial motivation was merely to follow up some observations that seemed curious at the time. Our curiosity is now satisfied, and we do not intend to pursue the matter further. Since the main role of the TG is probably to decrease the mean correlation length within the crystal, other methods, *e.g.* ultrasonics, for doing this should also be explored.

We are indebted to Dr V. Gramlich for helpful discussion and to Professor K. N. Trueblood for his critical and constructive comments on the manuscript.

### References

BATTERMAN, B. W. (1964). *Phys. Rev.* **134**, 1354–1356.
BECKER, P. (1977). *Acta Cryst* A**33**, 243–249.
BECKER, P. & COPPENS, P. (1974). *Acta Cryst.* A**30**, 129–147.
CHANDRASEKHAR, S. (1956). *Acta Cryst.* **9**, 954–956.
CHANDRASEKHAR, S., RAMASESHAN, S. & SINGH, A. (1969). *Acta Cryst.* A**25**, 140–142.
COOPER, M. J. & ROUSE, K. D. (1970). *Acta Cryst.* A**26**, 214–223.
COPPENS, P. & HAMILTON, W. C. (1970). *Acta Cryst.* A**26**, 71–83.
DARWIN, C. G. (1922). *Philos. Mag.* **43**, 800–829.
DENNE, W. A. (1972) *Acta Cryst.* A**28**, 192–201.
IZRAEL, A. & PETROFF, J. F. (1973). *Acta Cryst.* A**29**, 541–544.
KATAGAWA, T. & KATO, N. (1974). *Acta Cryst.* A**30**, 830–836.
KATO, N. (1976). *Acta Cryst.* A**32**, 453–466.
LAWRENCE, J. L. (1977). *Acta Cryst.* A**33**, 232–234.
MATHIESON, A. MCL. (1977). *Acta Cryst.* A**33**, 133–136.
PENNING, P. & POLDER, D. (1961). *Philips Res. Rep.* **16**, 419–440.
SCHNEIDER, J. R. (1977). *Acta Cryst.* A**33**, 235–243.
SEILER, P., DOBLER, M. & DUNITZ, J. D. (1974). *Acta Cryst.* B**30**, 2744–2745.
THORNLEY, F. R. & NELMES, R. J. (1974). *Acta Cryst.* A**30**, 748–757.
ZACHARIASEN, W. H. (1967). *Acta Cryst.* **23**, 558–564.


*Acta Cryst.* (1978) A**34**, 336–341

# A Neutron Diffraction Study of the Wavelength Dependence of Extinction in $UO_2$

BY M. SAKATA,* M. J. COOPER, K. D. ROUSE AND B. T. M. WILLIS

*Materials Physics Division, AERE Harwell, Oxfordshire OX11 0RA, England*

(*Received* 7 *August* 1977; *accepted* 21 *October* 1977)

Neutron diffraction measurements have been carried out on a single crystal of $UO_2$ examined at four different wavelengths; 0·85, 1·12, 1·54 and 1·84 Å. The Bragg intensities were analysed for the wavelength dependence of extinction using both the Cooper–Rouse and the Becker–Coppens formulations. Both treatments showed that the crystal is of type I (*i.e.* $r \gg \lambda g$, where $r$ is the domain radius, $\lambda$ the wavelength and $g$ the mosaic-spread parameter). The value of $g$ is the same, within one standard deviation, for each wavelength; its magnitude is appreciably less than for other crystals ($SrF_2$,ZnS,ZnTe,KCl) which have been examined by neutron diffraction at a number of wavelengths. Keeping the isotropic temperature factor for uranium fixed at 0·28 Å$^2$, the value of 0·55 ± 0·02 Å$^2$ is derived for the temperature factor of oxygen. There are no significant differences between the values of the extinction parameters and temperature factors obtained using the Cooper–Rouse treatment and the Becker–Coppens treatment based on either a Gaussian or a Lorentzian mosaic-spread distribution.

## 1. Introduction

Currently there is much interest in measuring neutron Bragg intensities using a fixed scattering angle $2\theta$ and a variable wavelength $\lambda$. Pulsed sources such as the Harwell LINAC adopt this arrangement instead of the more conventional system with a variable scattering angle and fixed wavelength. It is, therefore, of much interest to examine extinction effects as a function of wavelength. In this paper we report measurements of the neutron Bragg intensities of a single crystal of $UO_2$ at four different wavelengths: 0·85, 1·12, 1·54 and 1·84 Å. The measurements have been analysed using two theories of extinction: those due to Cooper & Rouse (1970) and Becker & Coppens (1974*a*,*b*, 1975). We show that, for this sample, the two theories give essentially the same results and cannot, therefore, be distinguished from one another. To distinguish the two theories requires measurements carried out on a crystal with larger secondary extinction than the $UO_2$ crystal, or on a crystal in which the extinction is determined by the domain radius rather than the mosaic spread (a type II crystal).

## 2. Cooper–Rouse theory

The Cooper–Rouse theory is based on that of Zachariasen (1967). The Zachariasen treatment of

* On leave from Nagoya University, Nagoya, Japan.